

## Snow gliding and loading under two different forest stands: a case study in the north-western Italian Alps

Davide Viglietti • Margherita Maggioni • Enrico Bruno  
Ermanno Zanini • Michele Freppaz

Received: 2012-06-15; Accepted: 2013-02-27  
© Northeast Forestry University and Springer-Verlag Berlin Heidelberg 2013

**Abstract:** The presence of a thick snowpack could interfere with forest stability, especially on steep slopes with potential damages for young and old stands. The study of snow gliding in forests is rather complex because this phenomenon could be influenced not only by forest features, but also by snow/soil interface characteristics, site morphology, meteorological conditions and snow physical properties. Our starting hypothesis is that different forest stands have an influence on the snowpack evolution and on the temperature and moisture at the snow/soil interface, which subsequently could affect snow gliding processes and snow forces. The aim of this work is therefore to analyse the snowpack evolution and snow gliding movements under different forest covers, in order to determine the snow forces acting on single trees. The study site is located in a subalpine forest in Aosta Valley (NW-Italy) and includes two plots at the same altitude, inclination and aspect but with different tree composition: Larch (*Larix decidua*) and Spruce (*Picea abies*). The plots were equipped with moisture and temperature sensors placed at the snow/soil interface and glide shoes for continuous monitoring of snow gliding. The recorded data were related to periodically monitored snowpack and snow/soil interface properties. Data were collected during two winter seasons (2009–10 and 2010–11). The snow forces on trees were analytically calculated either from snowpack data and site morphology or also from measured snow gliding rates. Different snow accumulations were observed under

the two different forest stands, with a significant effect on temperature and moisture at the snow/soil interface. The highest snow gliding rates were observed under Larch and were related to rapid increases in moisture at the snow/soil interface. The calculated snow forces were generally lower than the threshold values reported for tree uprooting due to snow gliding, as confirmed by the absence of tree damages in the study areas.

**Keywords:** snow/soil interface; temperature; water content; snow forces; trees

### Introduction

Snow forces are the result of glide and creep processes of the snowpack: a) snow gliding is the slow downhill motion of the snow on the ground mainly influenced by the roughness of the ground surface and the wetness of the lowermost boundary layer of the snow cover; b) snow creep is the result of settlement and internal shear deformation parallel to the slope (In der Gand and Zupancic 1966).

The snow gliding is strictly dependent on physical snow characteristics, overall depth, density and moisture, and on morphological features, overall slope angle and surface roughness (McClung and Larsen 1989; Jones 2004; Margreth 2007; Höller et al. 2009). In the first period of extensive research of glide processes and glide avalanches, Bader et al. (1939) found that the most important factors that have an effect on glide are slope, exposure, degree of surface roughness, temperature at the ground surface and the thickness and properties of the snow cover. They proposed that the primary action of these factors is their effect on the frictional conditions of the slide surface. Basal friction is obviously reduced by the presence of liquid water at the snow/soil interface (McClung and Clarke 1987). Also Clarke and McClung (1999) stated that gliding can occur if 1) the interface is smooth (e.g. bare rock or grassy vegetation), 2) the temperature at the snow/ground interface is at 0° C, guaranteeing the presence of free water at the interface, and 3) the slope angle is at least 15° for roughness typical of alpine ground cover. Moreover, the in-

Fund project: This study was supported by the Project “Forêts de protection: techniques de gestion et innovation dans les Alpes occidentales” within the Operational Program ALCOTRA Italy-France 2009–2012”.

The online version is available at <http://www.springerlink.com>

Davide Viglietti (✉) • Margherita Maggioni • Enrico Bruno •

Ermanno Zanini • Michele Freppaz

University of Torino - Dipartimento di Scienze Agrarie Forestali e Alimentari and NatRisk-LNSA, Via L. Da Vinci 44, 10095 Grugliasco (TO), Italy. Tel: +39 011 6708522, Fax: +39 011 6708692.

E-mail: [davide.viglietti@unito.it](mailto:davide.viglietti@unito.it)

Corresponding editor: Chai Ruihai

tensity of gliding rates is strictly related to increases in snow/soil interface temperature and moisture (Lackinger 1987; McClung and Larsen 1989; Clarke and McClung 1999; Newesely et al. 2000).

The wide-scale analysis of snow gliding intensity in alpine and subalpine areas has to take into account the land-use changing: the abandonment of pastures and the natural reforestation could cause a significant change on the ground roughness. In particular, Newesely et al. (2000) found that the abandonment of agriculture land may foster an increase of snow gliding rates due to the reduction of basal frictions.

Although forests can reduce the snow gliding intensity (Leitinger et al. 2008) by preventing snow accumulation and homogeneous snow distribution due to interception and falling of snow from the crowns (Höller 1995, 2001), it is not possible to totally exclude snow gliding in forest. Snow gliding might have significant effects on forest plants; in particular, juvenescent trees might be uprooted from the ground or the growth of young plants might be strongly affected by the snow forces (In der Gand 1978). According to these evidences, Höller et al. (2009) evaluated, with different approaches, the snow gliding rates in an Austrian subalpine stand of small trees (*Pinus cembra*, *Larix decidua* and *Picea abies*). In the same work, snow forces measured in field, and back-calculated with different equations, were compared to the forces necessary to uproot the young trees: the authors reported that forces equal to 950 N and 3500 N can uproot juvenescent trees with a diameter of 0.02 m and 0.045 m, respectively.

The study of the snow gliding phenomenon in forests is rather complex because it is influenced not only by forest features (species, crown, diameter and density), but also by topography (slope angle, morphology, aspect), meteorological characteristics (air temperature, rain on snow events) and snowpack structure. Moreover, the impact of snow forces on trees depends on the forest characteristics itself, and could lead to different consequences in term of tree stability.

The aim of this work was to analyse the snowpack evolution and snow gliding movements under different forest covers, namely Larch (*Larix decidua*) and Spruce (*Picea abies*) stands, in order to determine the snow forces acting on trees of different species and diameters. In particular, we aim at evaluating the influence of physical properties as temperature and moisture at the snow/soil interface on snow gliding processes, and consequently on snow forces.

## Materials and method

### Study site

As this research was developed within the project “Forêts de protection: techniques de gestion et innovation dans les Alpes occidentales” (Protection forests: management and innovation techniques in the western Alps) in the frame of the Operational Program ALCOTRA Italy-France (2009–2012), the study site was chosen within a snow avalanche protection forest. Located in the

Municipality of Brusson, in the Aosta Valley Region (North Western Italian Alps), at an elevation of 1950 m a.s.l., the site is characterized by a south aspect and a mean slope angle of about 40°. The coniferous mixed forest of the study site is mainly composed by larch (*Larix decidua*), spruce (*Picea abies*) with a lower presence of pine (*Pinus uncinata*). The lower part of the forest was reforested in 1940, in order to protect the village beneath, and it was grazed.

The climate of the area is continental humid subarctic, with a mean annual air temperature equal to + 4 °C and a mean annual precipitation equal to 718 mm. The mean annual snow depth is 175 cm (historical dataset from 1913 to 2001, Mercalli et al. 2003).

Two adjacent plots (40x40 m), located at the same elevation and aspect, were chosen (Fig. 1): a) one within a larch stand (Larch plot) and b) one within a spruce stand (Spruce plot). By counting all trees in each plot (with stem diameter > 5 cm) the average stem density was determined equal to 300 stems/ha for both plots. The crown canopy, measured as crown projection, amounted to 60% for the Larch plot and 65% for the Spruce plot. The average stem diameter was 40 cm and most of the trees were included in the range 30–40 cm (10 cm interval). The natural regeneration was generally scarce.

### Data collection

At the snow/soil interface (2 cm deep in the soil organic horizon) each plot was equipped with thermistor probes, with accuracy of ±0.1 °C, (MadgeTech®) and volumetric moisture probes, which measure the dielectric constant of the media through the utilization of capacitance/frequency domain technology, with accuracy of ±3% VWC, (EC-5MadgeTech). Temperature and moisture measured at snow/soil interface were named respectively as Ti and Mi, while the increase of Mi over time was named wetting rate.

Moreover, two glide shoes connected to potentiometers (Sommer®) (Fig. 2) as developed by In der Gand (1954) and successively applied by other scientists (e.g. Leitinger et al. 2008; Höller et al. 2009), were placed in each plot at a minimum distance of 5 m below the first upwards tree. The potentiometers were calibrated in order to convert the electric signal registered by the snow shoes into downward movement (mm/day), caused by snow gliding. All sensors were connected with a central data logger (Datataker® DT-80) supplied by a long duration battery and set to record the different parameters every 15 minutes. The electric wires were cabled underground in order to minimize their effect on the surface roughness.

The meteorological data were acquired by an automatic snow and weather station (Gressoney-Weissmitten 2038 m a.s.l.) located 3 km apart from the study site (belonging to the Ufficio Centro Funzionale of the Aosta Valley Region).

The snowpack physical characteristics (snow depth - $H_s$ -, snow density - $\rho$ -, grain types and size, snow temperatures, hand hardness index) were measured monthly, following standard international methods (Fierz et al. 2009): 8 snow profiles in winter 2009–2010 and 3 snow profiles in winter 2010–2011 were de-

scribed in both plots (Table 1). The damages to the trees were evaluated in the field by observations of eventual uprooted trees

and broken branches at the end of winters.

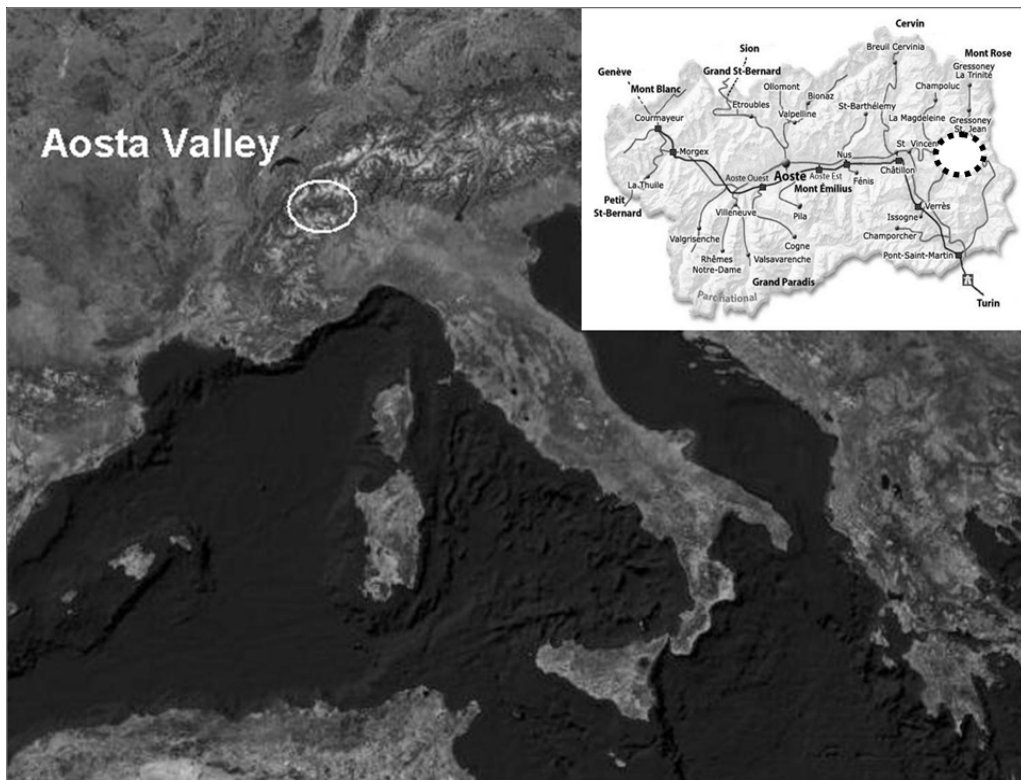


**Fig. 1** Localization of the study site and of the two selected plots.

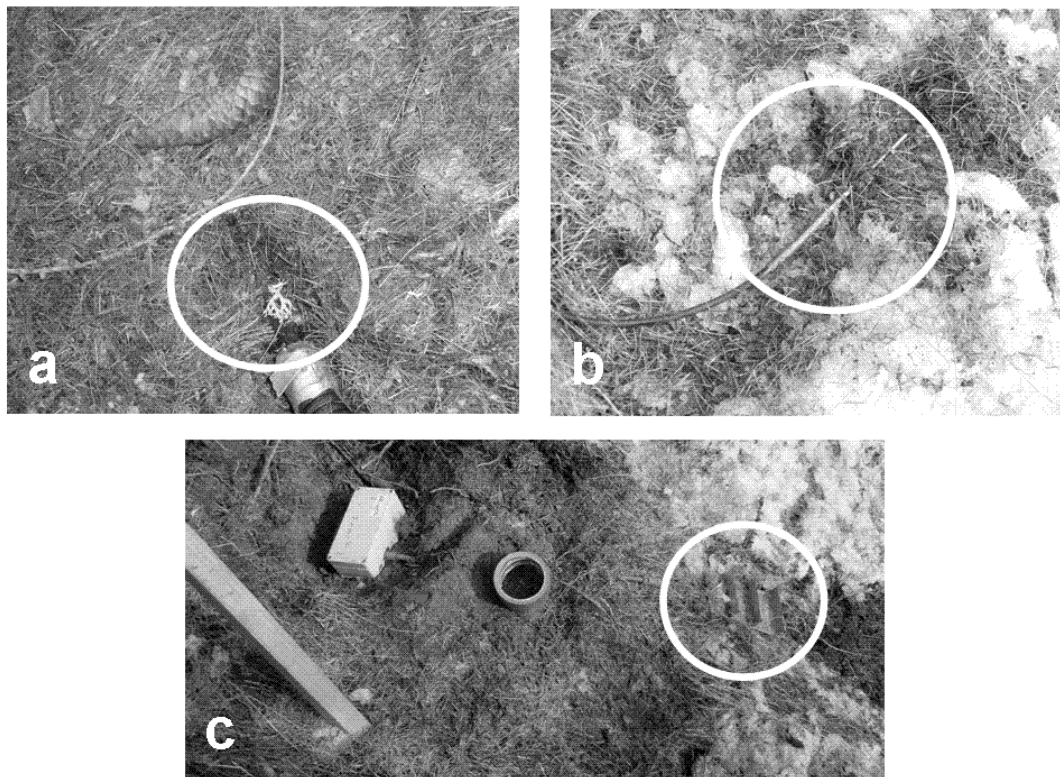


**Fig. 2** Moisture (a) and temperature (b) sensors, and a glide shoe (c), connected to the potentiometer, used in this study.

**Table 1.** Physical snow properties - according to Fierz et al. (2009) - measured in the field during winter 2009–2010 (8 snow profiles) and 2010–2011 (3 snow profiles), under Larch and Spruce plots.

Parameter	2009–2010		2010–2011	
	Larch	Spruce	Larch	Spruce
Maximum value of snow depth (cm)	60	66	28	22
Dominant grain type	FCso, MFpc	FCso, DHcp	RGsr	RGsr
Maximum grain size (mm)	2.5	4	1.5	1.5
Mean hand hardness Index	3	4	3	2
Mean snow density ( $\text{kg}\cdot\text{m}^{-3}$ )	277	229	220	270
Dominant grain type in the basal layer	FCso, DHcp	DHcp	FCso	FCso
Mean snow/soil interface temperature ( $^{\circ}\text{C}$ )	-3.8	-2.1	-1.1	-1.8
Date of snowpack isothermal condition	March 11 <sup>rd</sup>	March 19 <sup>rd</sup>	March 14 <sup>rd</sup>	March 20 <sup>rd</sup>

Note: FCso means solid faceted particles; MFpc means rounded polycrystals; DHcp means hollow cups; RGsr means small rounded particles.

Data collection was done from the middle of November 2009 until the end of April 2010 (called winter 2009–2010) and from the middle of November 2010 until the end of April 2011 (called winter 2010–2011). The seasons were identified according to meteorological quarterly subdivision: fall included September, October, November; winter included December, January and February; spring included March, April and May.

#### Calculation of snow forces

The calculation of snow forces on stems was done following the approach used by Höller et al. (2009). In particular, two different methods were applied by using a) empirical equations (Margreth et al. 2007) and b) snow gliding data recorded with glide shoes (Mc Clung and Larsen, 1989). We calculated snow forces for different stem diameters (0.02, 0.05, 0.1, 0.2, 0.3, 0.4, 0.5 m) in order to consider the real diameter distribution observed in the field and to compare our results with the available literature.

#### Snow pressure according to the Swiss guidelines

Margreth et al. (2007) applied the Swiss Guidelines with some improvements in order to calculate snow pressure on cableway masts. The snow pressure was calculated with the following equation (Eq. 1):

$$S'_N = \rho g (H_S^2 / 2) K N \quad (1)$$

where:  $S'_N$  is the snow pressure component in the line of slope per meter run of the supporting surface along the contour line [ $\text{kN}\cdot\text{m}^{-1}$ ],  $\rho$  is the density of the snow cover [ $\text{t}\cdot\text{m}^{-3}$ ],  $g$  is the gravitational acceleration [ $\text{ms}^{-2}$ ],  $H_S$  is the vertical snow depth [m];  $K$  is the creep factor dependent on the slope inclination  $\psi$  and the density  $\rho$ , and  $N$  is the glide factor.

In Margreth et al. (2007) the  $K$  factor was associated to fixed snow density values. We interpolated those values in order to calculate the exact  $K$  factor from the snow density that we measured in the field ( $y = 0.73x + 0.547$ ,  $r^2 = 0.991$ , where  $y$  corresponds to  $K/\sin 2\psi$  and  $x$  to  $\rho$ ). After that,  $K/\sin 2\psi$  was multiplied by  $\sin 2\psi$  (where  $\psi$  corresponds to the inclination of the study site).

In Margreth et al. (2007), the  $N$  factor depends on the ground roughness and aspect: it increases from WNW-N-ENE to ENE-S-WNW and it is inversely related to the ground roughness. Forest is not a determining parameters in the choice of  $N$ . Therefore, in our forested plots, we used the ground class 1, assuming that stems determined a high surface roughness (more than boulders). The study site was included in the ENE-S-WNW aspect class, because it is located on a South slope. Finally, we chose a glide factor  $N$  equal to 1.3.

Equation 1, which is valid only for infinitely long planes, was integrated, as suggested by Margreth et al. (2007), with a coefficient ( $\eta_F$ ), in order to consider the end-effect forces on narrow obstacles.  $\eta_F$  was calculated with the following equation (Eq. 2):

$$\eta F = 1 + c(D/W) \quad (2)$$

where:  $D$  is the snow thickness (calculated as  $H_S \cos \psi$ , where  $H_S$  is the vertical snow depth measured in the field and  $\psi$  is the slope angle);  $W$  is the width of the structure (that corresponded to the stem diameter);  $c$  is a non-dimensional coefficient and depends on the snow gliding intensity. It is usually deduced from the Swiss Guidelines. We used the smallest coefficient ( $c = 0.6$ ) because the snow gliding is typically low in dense forest areas (Höller 2001).

Subsequently, equations 1 and 2 were joined in Eq. 3:

$$S'_{N,M} = \rho g (H_S^2 / 2) K N \eta_F (W/D) \quad (3)$$

Finally, the snow pressure  $S'_{N,M}$  was multiplied by the different stem diameter classes in order to compare our results, in term of forces, with those presented by Höller et al. (2009).

#### Snow pressure according to Mc Clung and Larsen (1989)

This method considered the snow gliding rates directly measured in the field to determine principal stress on structures in dependence of the stagnation depth:

$$\sigma = \{ [2/(1-\nu)] [(d'/D) + (L/H_s)] \} 0.5 \rho g \text{disn} \psi + 0.5 [\nu/(1-\nu) \rho g D \cos \psi]$$

where:  $\sigma$  is the maximal principal stress of the snow on a structure [ $\text{Nm}^{-2}$ ],  $\nu$  is the Poisson coefficient deduced from Salm et al. (1971). We used  $\nu = 0.1$  that corresponds to a mean snow density of  $250 \text{ kg}\cdot\text{m}^{-3}$ , equal to the density we measured in our plots;  $L/H_s$  is a dimensionless creep parameter calculated by McClung and Larsen (1989) equal to  $0.27 + (\nu/12)$ ,  $D$  is the snow thickness,  $\rho$  is the snow density measured in the field [ $\text{kg}\cdot\text{m}^{-3}$ ],  $g$  is the gravitational acceleration [ $\text{m}\cdot\text{s}^{-2}$ ],  $\psi$  is the slope angle, and  $d'$  is the stagnation depth.

The stagnation depth is a fundamental parameter to formulate the boundary condition at the snow/soil interface. We calculated the stagnation depth  $d'$  from the measured snow gliding rates using Equation 5 (McClung 1974):

$$d' = [\mu V_g] / [2(1-\nu) \rho g D \sin \psi]$$

where:  $\mu$  is the viscosity, equal to  $10^{11} \text{ Pa}$  for snow,  $V_g$  is the snow gliding velocity [ $\text{mm/day}$ ]. According to Hoeller (2009) we used the maximum daily snow gliding rate recorded during winters 2009–2010 and 2010–2011;  $\nu$  is the Poisson coefficient.

#### Statistical analysis

Descriptive statistics were used to analyzed meteorological pattern, snow physical characteristics, and snow gliding data. Correlation analysis between temperature and moisture at snow/soil interface and between air temperature and temperature and moisture at snow/soil interface were carried out using the SPSS 12.0 for Windows (SPSS, 2003).

## Results and discussion

### Winter 2009–2010

#### Meteorological patterns

The mean air temperatures was  $-5.2^\circ\text{C}$  with a minimum value of  $-14.3^\circ\text{C}$  registered on 19th of December 2009 (Fig. 3a). This season was characterized by one short mild period, from December 6th to 10th, when the air temperature reached positive values with a maximum of  $+3.9^\circ\text{C}$ . The mean daily air temperature became constantly positive after 20th of April 2010. The automatic weather station recorded a cumulative precipitation equal to 330 mm of snow water equivalent (SWE) for the whole winter. The maximum snow depth (135 cm) was reached on 2nd of April 2010.

The cumulative snowfall was lower than the 75 years historical mean (488 mm of SWE) reported by Mercalli et al. (2003); in particular, the difference was remarkable especially during January, February and April.

#### Snow physical characteristics

In the *Larch plot*, the measured snow depth reached a maximum of 60 cm on January 13th. The snow density ranged between  $184 \text{ kg}\cdot\text{m}^{-3}$  (on January 13th) and  $362 \text{ kg}\cdot\text{m}^{-3}$  (on March 3rd). The first snow profile (December 9th) showed an isothermal snowpack with a basal layer characterized by slush crystals (MFsl). From the middle of December to the middle of February the thermal gradient increased and determined the formation of faceted crystals (MCso) and depth hoar (DHcp). In March the snowpack was again mostly at isothermal conditions with a predominance of melt-freeze crusts (MFcr).

The maximum snow depth measured in the *Spruce plot* (66 cm) was reached on February 2nd. The snow density ranged between  $163 \text{ kg}\cdot\text{m}^{-3}$  (on December 22nd) and  $296 \text{ kg}\cdot\text{m}^{-3}$  (on March 3rd). From the middle of December till the middle of February the thermal gradient increased and determined the formation of faceted crystals (MCso) and depth hoar (DHcp). In March the snowpack reached isothermal conditions with a predominance of cluster rounded crystals (MFcl).

#### Temperature and moisture at the snow/soil interface

In the *Larch plot*, the temperature at the snow/soil interface  $T_i$  (Fig. 3b) was positive until December 10th, except on November 29th, when a first freezing event occurred (daily average  $T_i = -1.3^\circ\text{C}$ ). Later  $T_i$  remained below  $0^\circ\text{C}$  from the middle of December until the end of March. A sharp increase of  $T_i$  (which reached  $0^\circ\text{C}$ ) was observed on December 26th, January 1st, February 19th, March 3rd and March 18th. The moisture at the snow/soil interface  $M_i$  (Fig. 3c) was correlated with soil ( $r = +0.498$ ;  $p < 0.01$ ) and air temperatures ( $r = +0.418$ ;  $p < 0.01$ ). The maximum values were recorded several times during this winter season and in particular on December 8th (21%), with a wetting rate of 2%/day for 11 days, on December 25th (20%), with a wetting rate of 15% in one day and on February 26<sup>th</sup> (22%) with a wetting rate of 5%/day for 2 days. The period between the beginning of January and the middle of February was characterized by a constant value of  $M_i$  close to 10%.

In the *Spruce plot* the temperature at the snow/soil interface  $T_i$  (Fig. 3b) was positive until November 29th ( $T_i = -0.8^\circ\text{C}$ ). Later  $T_i$  remained constantly below  $0^\circ\text{C}$  from the middle of December until the end of March. The moisture at the snow/soil interface  $M_i$  (Fig. 3c) showed remarkable oscillations until the beginning of January, with 3 maximum values recorded on November 16<sup>th</sup> (14%), with a wetting rate equal to 2.5%/day for 4 days, on December 11th (15%), with a wetting rate of 1%/day for 14 days and on December 25th (13%), with a wetting rate of 6.5%/day for 2 days. Later,  $M_i$  remained constant (around 5%) until March 19th. From March 19th to 24th a remarkable increase was observed (+3.2%/day), reaching a moisture value of 21.3% on March 24th.  $M_i$  was correlated with  $T_i$  ( $r = +0.641$ ;  $p < 0.01$ ) and air temperature ( $r = +0.631$ ,  $p < 0.01$ ).

#### Snow gliding

While no snow gliding events were observed in the *Spruce plot*, under *Larch*, only a single event of snow gliding occurred (Fig.

3d) between December 1st and 14th after the first seasonal snowfall (30 cm of fresh snow). In this period,  $M_i$  rose by 20% and the dominant grain type in the basal layer observed on December 9<sup>th</sup> was slush (MFS<sub>l</sub>), indicating a consistent presence of liquid water. The cumulative movement of the glide shoes was equal to 19 mm, with an average daily snow gliding rate of 1.9 mm/day for 10 days and a maximum daily snow gliding rate of 3.9

mm/day. The volumetric moisture at the snow/soil interface increased with a wetting rate +3.8%/day for 5 days.

From the middle of December until the end of the monitoring period, no snow gliding was observed, although a significant increase of snow/soil interface temperature and moisture was recorded at the end of March (wetting rate of +1.5% day for 12 days).

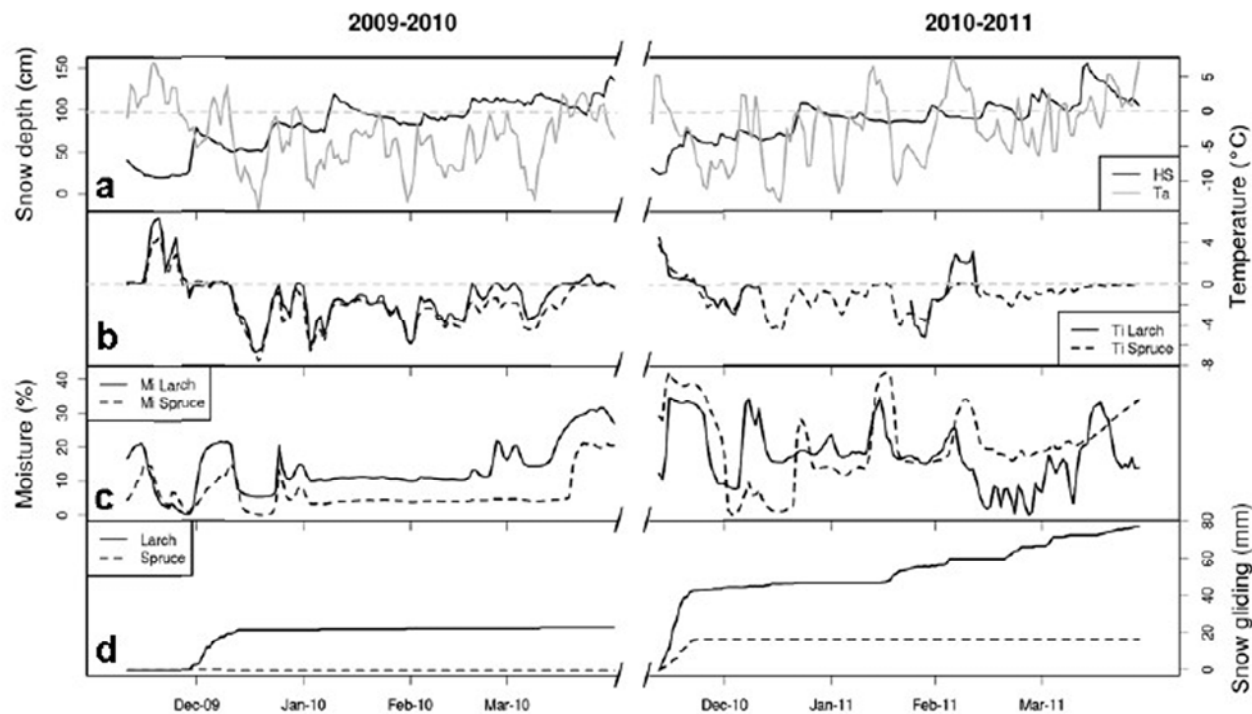


**Fig. 3** Snow depth and air temperature measured by the automatic snow and weather station (a);  $T_i$  (b)  $M_i$  (c) and snow gliding (d) in each plot recorded in both winters (2009-2010 and 2010-2011) when the study site was snow-covered.

#### Snow forces

In the *Larch plot*, the snow forces on stems with different diameters, calculated by Equation 3, as in Margreth et al. (2007), ranged from 3 to 290 N (Fig. 4a). Two maximum occurred at the middle of January ( $H_S = 60$  cm and  $\rho_{\text{snow}} = 184 \text{ kg}\cdot\text{m}^{-3}$ ) and at the beginning of March ( $H_S = 47$  cm and  $\rho_{\text{snow}} = 362 \text{ kg}\cdot\text{m}^{-3}$ ).

We also calculated the snow forces as in Mc Clung and Larsen (1989), corresponding to the single snow gliding episodes (beginning of December), when a movement of 3.9 mm/day was registered by the snow shoes. The necessary input values for the snow depth and density were taken from the snow pit dug on 9<sup>th</sup> of December:  $H_S = 25$  cm and  $\rho_{\text{snow}} = 250 \text{ kg}\cdot\text{m}^{-3}$ . The resulting forces ranged from 11 to 284 N on the different stem diameters (Table 2).

In the *Spruce plot* the snow forces on stems with different diameters, calculated by Equation 3, as in Margreth et al. (2007), ranged from 2 to 361 N (Fig. 4b). A maximum was observed at the middle of February, when  $H_S$  was equal to 66 cm and  $\rho_{\text{snow}} = 231 \text{ kg}\cdot\text{m}^{-3}$ .

During winter 2009–2010, it was not possible to calculate the snow forces as in Mc Clung and Larsen (1989), as no snow gliding event occurred under Spruce.

**Table 2.** Snow forces values calculated according to Mc Clung and Larsen (1989) for the different stem diameter classes under Larch (L) and Spruce (S) in winters 2009-2010 and 2010-2011.

Date and snow gliding rates	Forces at different diameter classes (N)						
	0.02 m	0.05 m	0.1 m	0.2 m	0.3 m	0.4 m	0.5 m
2009-2010 <sup>a</sup>	Larch plot						
December 4 <sup>th</sup> , 3.9 mm/day	11.37	28.43	56.86	113.72	170.58	227.47	284.30
2010-2011	Larch plot						
November 17 <sup>th</sup> , 1.4 mm/day	7.38	18.46	36.92	73.83	110.75	147.66	184.54
January 20 <sup>th</sup> , 0.4 mm/day	2.55	6.39	12.77	25.55	38.32	51.10	63.87
March 03 <sup>rd</sup> , 0.1 mm/day	1.82	4.54	9.08	18.17	27.25	36.34	45.42
Spruce plot							
November 19 <sup>th</sup> , 0.4 mm/day	2.62	6.56	13.11	26.22	39.33	52.45	65.56

<sup>a</sup> In 2009–2010 no snow gliding occurred in the Spruce Plot.

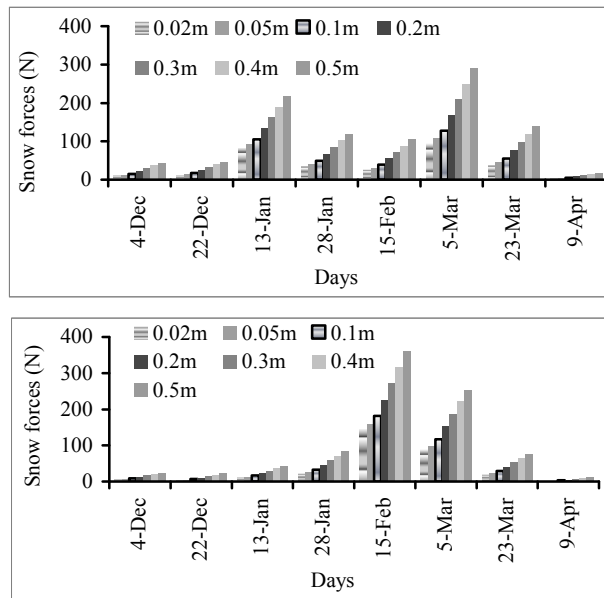


**Fig. 4** Snow forces calculated according to Margreth et al. (2007) at different stem diameters during winter 2009–2010 in the Larch (a) and Spruce plots (b).

Winter 2010–2011

#### Meteorological pattern

In winter 2010–2011 the mean air temperature was  $-3.0^{\circ}\text{C}$  with a minimum value of  $-14.3^{\circ}\text{C}$  recorded on December 18th (Fig. 3). Winter 2010–2011 was characterized by frequent and longer mild periods than winter 2009–2010. The mean daily air temperature became constantly positive from March 22nd. Concerning precipitations, the automatic weather station recorded a cumulative precipitation equal to 298 mm of snow water equivalent (SWE). The maximum snow depth (156 cm) was reached on March 17th.

The cumulative snowfalls were lower than the 75 years historical data (488 mm of SWE) reported by Mercalli et al. (2003): in particular, the difference was remarkable especially during January, February and April.

#### Snow physical characteristics

In the *Larch plot*, a maximum snow depth equal to 28 cm was observed on December 2nd. The snow density ranged between  $146 \text{ kg}\cdot\text{m}^{-3}$  (on December 2nd) and  $340 \text{ kg}\cdot\text{m}^{-3}$  (January 18th). The first snow profile showed a kinetic metamorphism with the presence of faceted crystals (FCso), which we found also on January 18<sup>th</sup>. Moreover the dominant grain type in the basal layer was rounded polycrystals (MFpc) suggesting a previous presence of liquid water. On March 23rd a prevalence of cluster rounded crystals (MFcl) was observed.

In the *Spruce plot*, the maximum snow depth was observed in the last snow profile (28 cm) on March 23rd. The snow density ranged between  $230 \text{ kg}\cdot\text{m}^{-3}$  (on December 2nd) and  $320 \text{ kg}\cdot\text{m}^{-3}$  (January 18th). The first snow profile revealed the beginning of kinetic metamorphism, with faceted crystals (FCso) as prevalent crystals; moreover a thin ice layer (IFil) was observed at the bot-

tom of the snowpack. On March 23rd a prevalence of rounded crystals (RGl) was observed.

#### Temperature and moisture at the snow/soil interface

The temperature sensors in the *Larch plot* were repeatedly damaged by rodents, therefore the measurements were interrupted. The recorded  $T_i$  values ranged only from November to December and from the end of January until the middle of February (Fig. 3b).

The moisture at the snow/soil interface  $M_i$  (Fig. 3c) was characterized by 4 sharp increases: the first (34%) occurred from November 14th to 16th (wetting rate: +12%/day); the second (34%), occurred from December 5th to 9th (wetting rate: +9%/day); the third (37%) occurred from January 13th to 16th (wetting rate: +5%/day); the fourth (32%), occurred from March 13th to 20th (wetting rate: +4%/day). On the contrary,  $M_i$  strongly decreased (-25%) from November 21st until December 4th, with a water depletion rate equal to -1.8%/day.  $M_i$  was positively correlated with the air temperature ( $r = +0.256$ ;  $p < 0.01$ ).

In the *Spruce plot* the temperature at the snow/soil interface  $T_i$  (Fig. 3b) was constantly negative from November 24th until March 3rd, except three periods when it reached  $0^{\circ}\text{C}$  (December 8th, January 14th to 18th and February 6th to 11th). Two minimum values were reached, on December 18th ( $-4.6^{\circ}\text{C}$ ) and January 21th ( $-4^{\circ}\text{C}$ ). When the snow/soil interface temperature increased, also the moisture  $M_i$  did ( $r = +0.650$   $p < 0.01$ ), and the maximum values, 42%, 49% and 33%, were reached on November 16th, January 15th and February 9th, respectively (Fig. 3c). Instead, the minimum water content measured in the Spruce plot (0%) was reached at the beginning of December when the snow/soil interface was frozen.

#### Snow gliding

In the *Larch plot*, several snow gliding events were measured with a cumulative movement of 77 mm (Fig. 3d). The first snow gliding event was recorded after the first snowfall (25 cm) at the end of November. From November 13th to 23rd a cumulative movement of 43 mm was recorded. In this period,  $T_i$  was positive (daily average  $T_i = 1.4^{\circ}\text{C}$ ) and a remarkable snow/soil moisture increase (+7.4%/day for 3 days) occurred. The highest snow gliding rate (1.4 mm/day) was measured on November 17th. In the snow profile dug closer in time to this snow gliding event (December 2nd) the dominant grain type in the basal layer was rounded polycrystals (MFpc), indicating that melt-freeze metamorphism occurred, with the presence of some liquid water. Until the middle of January, the snow gliding rates decreased, with a cumulative value equal to 5.8 mm. From January 19th till April 4th other snow gliding events were observed (with a cumulative movement of 29 mm): the highest daily movement was recorded on January 20th (0.4 mm/day) and on March 3rd (0.1 mm/day), after a significant increase of  $M_i$  (respectively +2.4/day for 7 days and +8.7 in one day). Especially on January 18th an increase in snow moisture across the snow pack was observed: the basal layer contained a significant amount of liquid water. No snow gliding was observed from February 6th until 16th because the study plot became snow free.

In the *Spruce plot*, only a single snow gliding event was observed, after the first snowfall, with a cumulative displacement of 16 mm, from the 13th to the 25th November. In the snow profile dug closer in time to this snow gliding event (December 2nd) a thin ice layer (IF1) was observed at the bottom of the snowpack indicating a previous presence of some liquid water at the snow/soil interface. The highest snow gliding rate (0.4 mm/day), was measured on November 19th, after a significant increase of the volumetric moisture (+4.75/day for 3 days). From the end of November until the end of the monitoring period, no snow gliding was observed, despite several increments at the snow/soil interface moisture were recorded.

#### Snow forces

In the *Larch plot*, the snow forces on stems with different diameters calculated by Equation 3 (as in Margreth et al., 2007) ranged from 0.5 to 29 N (Fig. 5a). The snow forces decreased from the beginning of December ( $H_s = 28$  cm;  $\rho_{\text{snow}} = 146$  kg·m<sup>-3</sup>) to the beginning of January ( $H_s = 10$  cm;  $\rho_{\text{snow}} = 340$  kg·m<sup>-3</sup>) and then remained almost constant until the end of the season. Also according to Mc Clung and Larsen (1989), the snow forces decreased across the season since the maximum snow gliding rate, 1.4 mm/day, was observed on November 17th and the minimum one, 0.1 mm/day, was measured on March 3rd. The resulting forces ranged from 2 to 184 N (Table 2).

In the *Spruce plot*, the snow forces on stems with different diameters calculated by Equation 3 (as in Margreth et al., 2007) ranged from 0.6 to 21 N (Fig. 5b). The snow forces were almost constant until the beginning of January ( $H_s = 11$  cm;  $\rho_{\text{snow}} = 320$  kg·m<sup>-3</sup>) and then started to increase until the end of March ( $H_s = 28$  cm;  $\rho_{\text{snow}} = 260$  kg·m<sup>-3</sup>). We also calculated the snow forces as in Mc Clung and Larsen (1989), in correspondence of the single snow gliding episode (second half of November), when a movement of 0.4 mm was registered by the snow shoes. The necessary input values for the snow depth and density were taken from the snow pit dug on December 2nd:  $H_s = 20$  cm and  $\rho_{\text{snow}} = 232$  kg·m<sup>-3</sup>. The resulting forces ranged from 3 to 66 N on the different stem diameters (Table 2).

#### Comparison between Larch and Spruce plots

##### Snow physical characteristics

Tree species affect only some physical characteristics of the snowpack. In fact, the crystal type and dimension were similar both under Larch and Spruce stands. Instead, the snow depth evolution had a different pattern for the two sites: in mid winter, snowfalls generated a deeper snowpack in the Larch plot, because of the reduction of snow interception due to the absence of leaves in the winter period; on the contrary, in spring, the shadow effect due to the evergreen cover maintained a deeper snowpack and increased the snow duration under the Spruce plot. The same effect of crown interception was found by Gubler and Rychetnik (1991) and Motta (1995).

A higher average snow density was observed under Spruce, especially after snowfalls with mild air temperature, maybe due to the liquid water input from the melted snow intercepted by the

tree crowns. The snow density under Larch gradually increased and finally exceeded the values recorded under Spruce in spring, because of a more pronounced effect of solar radiation.

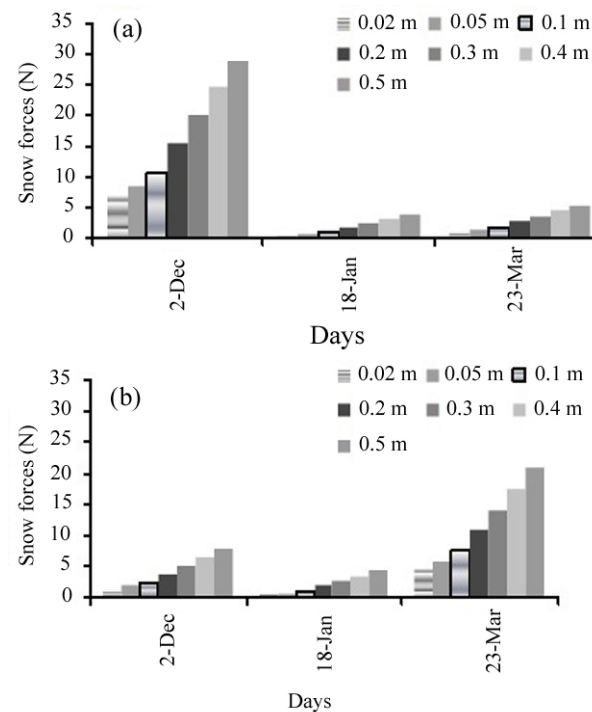


**Fig. 5** Snow forces calculated according to Margreth et al. (2007) at different stem diameters during winter 2010-2011 Larch (a) and Spruce (b) plots.

##### Temperature and moisture at the snow/soil interface

The mean snow/soil interface temperature was higher in the Larch than in the Spruce plots, especially during fall and spring. An explanation could be that the greater snow accumulation under Larch during early winter, when the soil was unfrozen, could have reduced the soil cooling rate, while the higher snow depth in the Spruce plot in late winter and spring could have determined a delay in the soil warming. Several authors (e.g. Brooks and Williams 1999; Freppaz et al. 2008) found that a snow depth approximately equal to 30–40 cm accumulating early in the winter season prevents soil from freezing.

Concerning the moisture at the snow/soil interface, we registered larger fluctuations in the Larch than in the Spruce plot. The reason might be that a lower crown cover allowed the radiation to reach the snowpack surface. This energy input increased the snow water content at the surface, which, due to a thin snowpack, was able to percolate downwards to the ground. On the contrary, in the Spruce plot, the larger crown cover lead to a lower influence of solar radiation and probably prevented the wetting front from reaching the soil.

##### Snow gliding

In both years the total snow gliding was higher under Larch than under Spruce. This fact was probably due to a lower snowpack basal friction under Larch than under Spruce, caused by great fluctuations of moisture at the snow/soil interface. The cumula-

tive snow gliding did not exceed 100 mm, as found also by Höller (2001) for a dense forest. Our results support the hypothesis that snow gliding is generally low when the canopy density is relatively high.

#### Snow forces

Generally, lower forces were calculated below Spruce than below Larch, due to the larger snow accumulation recorded in the latter site. We did not find any damages to young trees in both plots.

### General discussion

From our results, the snow/soil interface moisture significantly influenced the snow gliding processes. In particular, soil moisture at the snow/soil interface was related to the snow/soil interface temperature and both parameters ( $M_i$  and  $T_i$ ) were strongly regulated by air temperature. It seemed that the wetting rate at snow/soil interface was strongly influenced by air temperature and snow depth with a contrasting effect. In particular, we found that during early winter, when the snow cover was thin and homogeneous (mainly characterized by fresh snow) the volumetric moisture at the bottom increased in less than 24 hours under both plots after an increase of air temperature, as found also by Jones et al. (2001). Instead, in mid winter, when the snowpack was thicker and less homogeneous, after an increase of air temperature, the snow/soil interface moisture increased because of either a wetting front from the surface (which reached the bottom of the snowpack within a maximum of 4 days) and an increase of the snow/soil interface temperature (which reached 0 °C).

The volumetric moisture increase of a relatively dry snow/soil interface (10%–20%), seemed to be the most important factor influencing the snow gliding rates: in particular snow gliding was observed with wetting rates higher than 1.2%/day. The increase of volumetric moisture at the snow/soil interface might reduce the snowpack basal friction as suggested by several authors (In der Gand 1966; Clarke and Mc Clung 1999; Höller 2001; Margreth et al. 2007). The snow gliding events were mostly recorded, under both plots, during early winter and after the first snowfalls, when the soil was unfrozen, as observed also in long term studies, though conducted in open field (In der Gand and Zupancic 1966; Höller 2001). The first snow reaching the ground rapidly melted on a relatively warm soil ( $T_i > 0.5$  °C), thus determining an increase of moisture at the snow/soil interface, where the dominant crystal type was slush. During winter 2010–2011, snow gliding events were observed also during spring time. These phenomena were related to a sudden sharp air temperature increase, which consequently increased the snowpack moisture, followed by a strong air temperature decrease, as observed by McClung (1999). We could hypothesize that the snowpack became stiff and glided, as a block, on the liquid water film previously formed at the soil surface.

The snow forces calculated in this study were lower than the values reported in other studies conducted in the Alps (Höller et al. 2009). The differences could be attributed to the lower coefficients we used, because our study site was located under a ma-

ture forest stand, while the study site considered for example by Höller et al. (2009) was characterized by young trees. Moreover, our study site was characterized by lower snow density and thickness than the site studied by Höller et al. (2009).

With our data, the application of the method by Margreth et al. (2007), originally elaborated for the dimensioning of the cable-way masts, gave lower values than the method by Mc Clung and Larsen (1989), and the differences between the two methods became more significant with larger stem diameters. This difference highlights the need to directly measure the snow forces, by e.g. using load cells on the tree trunks, in order to validate the results obtainable with the two different methods.

The fact that we did not detect any damages to young trees, such as seasonal uproots and branch breakages, is in agreements with the low snow forces obtained with the two different methods. Our calculated snow forces were lower than the value of 950 N, found by Höller (2009), through pulling test, as the minimum force necessary to cause uprooting of young coniferous trees (*Larix decidua*, *Picea abies* e *Pinus cembra*), with stem diameters ranging from 2.5 to 5 cm.

However, the snow characteristics (e.g. density) and meteorological conditions (e.g. sharp increase of air temperature) recorded during the two winters considered in this study, caused significant snow gliding events, mainly during early winter, which contributed to determine non negligible snow forces on trees, though not producing damages.

Since the Climate change is expected to determine milder winter and more unstable snow cover in temperate mountain regions (Cooley 1990; IPCC 2007), it is possible to speculate a change also in the snow gliding processes. In particular, these areas could face a decline in snow cover (late snowpack accumulation and advance of snowmelt timing), an increase of snow density and more frequent episodes of rain on snow (Leung et al. 2004; Ye et al. 2008; Casson et al. 2010). Hence, the basal friction of the snowpack could be reduced by the liquid water on the basal portion of the snowpack and consequently amplify the rate of snow gliding. This fact might generate in future higher pressure on stems diminishing trees stability and therefore the forest protective function.

### Conclusion

In this work we evaluated the relationship between snow physical properties, microclimatic conditions at the snow/soil interface and the process of snow gliding during two winter seasons under two distinct forest covers, by means of continuous measurements and detailed field observations.

In particular we observed that:

(a) The snowpack physical evolution (e.g. snow density, snow depth) during the whole winter season was influenced by the tree species, due to the different crown interception of snowfall, and the different degree of exposure of the snowpack to the incoming solar radiation;

(b) The wetting rate at the snow/soil interface, associated to air temperature fluctuations, seemed to be the most important factor

influencing the snow gliding rates. The snow gliding rates were higher in early winter, when the first snowfall covers an unfrozen, warm soil. In this period, snow gliding was observed after the wetting of a relatively dry snow/soil interface;

(c) The highest snow gliding was measured under the Larch stand probably due to a lower basal friction at the snow/soil interface;

(d) The calculated snow forces were very low under both forest stands, if compared to other studies, mainly because the snow depth and the snow density were scanty during the study period.

### Acknowledgements

This study was possible thanks to the Project “Forêts de protection: techniques de gestion et innovation dans les Alpes occidentales” within the Operational Program ALCOTRA Italy-France 2009-2012). We thank Franca De Ferrari, Jean-Claude Haudemond, Antoine Brulpot, Franco Viglietti and Gianluca Filippa for the important contribution in field activities and data elaboration.

### References

Bader HR, Haefeli, E. Bucher, I. Neher, O. Eckel, Chr Thams. 1939. Der Schnee und seine Metamorphose (Snow and its Metamorphism). Beiträge zur Geologie der Schweiz, Geotechnische Serie, Hydrologie, Lieferung 3, Bern [English Translation by Snow, Ice Permafrost Research Establishment, Corps of Engineers, U.S. Army. Translation 14, January 1954], p.313.

Brooks PD, Williams MW. 1999. Snowpack controls on nitrogen cycling and export in seasonally snow-covered catchments. *Hydrol Process*, **13**: 2177–2190.

Casson NJ, Eimers MC, Buttle JM. 2010. The contribution of rain-on-snow events to nitrate export in the forested landscape of south-central Ontario, Canada. *Hydrol Process*, **24**:1985–1993.

Clarke J, Mc Clung D. 1999. Full depth avalanche occurrences caused by snow gliding, Coquihalla, British Columbia, *Canada J Glaciol* **45**(150): 539–546.

Cooley KR. 1990. Effects of CO<sub>2</sub>-induced climate changes on snowpack and streamflow. *Hydrol Sci J*, **35**: 511–522.

Freppaz M, Marchelli M, Celi L, Zanini E. 2008. Snow removal and its influence on temperature and N dynamics in alpine soils (Vallée d'Aoste - NW Italy). *J Plant Nutr Soil Sci*, **171**: 1–9.

Fierz C, Armstrong RL, Durand Y, Etchevers P, Greene E, McClung DM, Nishimura K, Satyawali PK, Sokratov SA. 2009. *The International Classification for Seasonal Snow on the Ground*. IHP-VII Technical Documents in Hydrology N°83, IACS Contribution N°1, UNESCO-IHP, Paris.

Gubler H, Rychetnik J. 1991. Effect of forests near the timberline on avalanche formation. In: *Snow Hydrology and Forest in High Alpine Areas* (Proceeding of Vienna Symposium, August 1991). IAHS Publ.205, 1991.

Höller P, Fromm R, Leitinger G. 2009. Snow Forces on forest plants due to creep and glide. *For Ecol Manag*, **257**: 546–552.

Höller P. 2001. Snow gliding and avalanches in a south-facing larch stand. *Intern Ass Hydrol Sci Publ*, **270**: 355–358.

in der Gand H, Zupancic M. 1966. Snowgliding and avalanches. In: *Scientific Aspects of Snow and Ice Avalanches* (Proceeding Davos Symposium, April 1965), pp.230–242 . IAHS n.69.

in der Gand H. 1954. Beitrag zum Problem des Gleitens der Schneedecke auf dem Untergrund. *Winterbericht Eidg. Inst. f. Schnee-und Lawinenforschung*, **17**:103–117.

In der Gand H. 1978. Verteilung und Struktur der Schneedecke unter Waldbäumen und im Hochwald. In: International Seminar on Mountain Forests and Avalanches. IUFRO Working Party on Snow and Avalanches. Davos: Swiss Federal Institute for Snow and Avalanche Research, pp.98–119.

Intergovernmental Panel on Climate Change (IPCC). 2007. Climate Change 2007: The Physical Science Basis. In: S. Solomon, D. Qin, and M. Manning (eds.), Working Group 1 Contribution to the Fourth Assessment Report of the IPCC. New York: Cambridge Univ. Press.

Jones HG, Pomeroy JW, Walker DA, Hoham RW. 2001. *Snow Ecology: an interdisciplinary examination of snow covered ecosystems*. Cambridge University Press, pp. 102–104.

Jones A. 2004. Review of glide processes and glide avalanche release. *Avalanche News* **69**: 53–60.

Lackinger B. 1987. Stability and fracture of the snow pack for glide avalanches. *Intern Ass Hydrol Sci Publ*, **162**:229–240.

Leitinger G, Höller P, Tasser E, Walde J, Tappeiner U. 2008. Development and validation of a spatial snow-glide model. *Ecol mod*, **211**: 363–374.

Leung LR, Qian Y, Bian X, Washington MW, Han J, Roads JO. 2004. Mid-century ensemble regional climate change scenarios for the western United States. *Climatic Change*, **62**: 75–113.

Margreth S. 2007a. *Defense structures in avalanche starting zones: Technical guideline as an aid to enforcement*. Environment in Practice no. 0704. Bern: Federal Office for the Environment; Davos: WSL Swiss Federal Institute for Snow and Avalanche Research SLF, p.136.

Margreth S. 2007b. Snow pressure on cableway masts: analysis of damages and design approach. *Cold Reg Sci Technol*, **47**: 4–15.

McClung DM, Clarke GKC. 1987. The effects of free water on snow gliding. *J Geoph Res*, **92**(7): 6301–6309.

McClung D, Larsen JO. 1989. Snow creep pressure: effect of structure boundary conditions and snowpack properties compared with field data. *Cold Reg Sci Technol*, **17**: 33–47.

Mercalli L, Catberro D, Montuschi S, Castellano C, Ratti M, Di Napoli G, Mortara G, Guindani N. 2003. Atlante Climatico della Valle D'Aosta (Climate Atlas for the Aosta Valley Region) (Eds. Società Meteorologica Subalpina), p.405.

Motta R. 1995. I larici delle Alpi occidentali: un problema ecologico selvicolturale. *SILVAE Pedemontis* **1**:7–16.

Newesely C, Spadiner P, Cernusca A, Tasser E. 2000. Effects of land-use changes on snow gliding processes in alpine ecosystems. *Bas Appl Ecol*, **1**: 61–67.

Salm B. 1977. Snow forces. *J Glaciol*, **19**(81): 67–100.

SPSS 2003. SPSS for Windows. Chicago: SPSS Inc..

Tasser E, Newesely C, Höller P, Cernusca A, Tappeiner U. 1999. Potential risks through land-use changes. In: ECOMONT. Ecological effects of land-use changes on European Terrestrial Mountain Ecosystems – Concepts and Results. Berlin, Wien: Blackwell Wiss.-Ver., pp. 218–224.

Tasser E, Tappeiner U, Cernusca A. 2001. Südtirols Almen im Wandel. Ökologische Folgen von Landnutzungsänderungen. European Academy of Bozen/Bolzano 28, Bozen, p 276.

Tasser E, Walde J, Tappeiner U, Teutsch A, Noggler W. 2007. Land-use changes and natural reforestation in the Eastern Central Alps. *Agr, Ecosyst, and Envir*, **118**: 115–129.

Valinger E, Lundqvist L. 1994. Reducing wind and snow induced damage in forestry. Swedish University of Agricultural Sciences. Department of Silviculture. Reports 37.

Viglietti D, Letey S, Motta R, Maggioni M, Freppaz M. 2010. Snow avalanche release in forest ecosystems: A case study in the Aosta Valley Region. *Cold Reg Sci Technol*, **64**(2): 167–173.

Ye H, Yang D, Robinson D. 2008. Winter rain on snow and its association with air temperature in northern Eurasia. *Hydrol Process*, **22**: 2728–36.